Journal of Applied Fluid Mechanics, Vol. 15, No. 4, pp. 1243-1253, 2022.
Available online at www.jafmonline.net, ISSN 1735-3572, EISSN 1735-3645.
https://doi.org/10.47176/jafm.15.04.33091

Aerodynamic and Aeroacoustic Performance of a Wing with Structured Surface Inspired by Owl's Wings

R. Harbi Monfared[1], M. Taeibi Rahni[†,2,3], M. Zareh[1], G. Ahmadi [4] and S. Etemadi Haghighi [1]

[1] *Department of Mechanical Engineering, Science and Research Branch, Islamic Azad University, Tehran, Iran*
[2] *Department of Aerospace Engineering, Sharif University of Technology, Tehran, Iran*
[3] *Khayyam Research Institute, Ministry of Science, Research and Technology, Tehran, Iran*
[4] *Department of Mechanical and Aeronautical Engineering, Clarkson University, Potsdam, NY, United States*

†*Corresponding Author Email: taeibi@sharif.edu*

(Received June 9, 2021; accepted March 9, 2022)

ABSTRACT

With the advent of various advanced materials, the idea of flying like birds has attracted considerable attention in recent years. In addition, aeroacoustics has become an important issue and is being widely studied. In this work, based on the shape of Owls' wings, an attempt was made to improve the aeroacoustic and aerodynamic performances of conventional aircraft wings. For this purpose, wings with different elements, namely, square, triangular, and semicircular, on their top surface were examined. In addition, three different spatial distributions of the elements according to the Owl's wings shape were considered. For incompressible airflow, aerodynamic and aeroacoustic parameters of wing with structured surfaces were investigated. Also, a wing with serrations was examined. The results indicate that wings with elements distributed starting from maximum section thickness and continuing up to the trailing edge are the most suitable case for both aerodynamic and aeroacoustic improvements. On the other hand, a two-sided serrated wing and a serrated wing in the trailing edge reduce the sound level significantly. In addition, the use of both elements and serrations delays wing stall and thus markedly increases the maximum lift coefficient.

Keywords: Aeroacoustics; Aerodynamics; UAVs; Owl; Wing with structured surfaces.

Nomenclature

c	speed of sound	T. E.	Trailing Edge
k	turbulence kinetic energy	URANS	Unsteady (Non-Stationary) Reynolds Averaged Navier-Stokes
l	flow length scale	α	model constant
P	total pressure	δ_{ij}	Kronecker delta
T_{ij}	Lighthill stress tensor	β^*	closure coefficient in turbulent kinetic energy equation
u	mean flow velocity	ε	turbulent dissipation rate
x_i	position vector	μ_t	eddy viscosity
L. E.	Leading Edge	ρ	mean density
L. M. T.	location of maximum wing section thickness	ρ_0	reference mean density
M. T.	maximum wing section thickness	$\rho v_i v_j$	Reynolds stress tensor
W. S. S.	wing with structured surface	ω	specific turbulence rate (or turbulence frequency)
S-A	Spalart–Allmaras	σ_{ij}	viscous stress tensor

1. INTRODUCTION

In the middle of the twentieth century, with the arrival of commercial jets, unwanted sound and noise became widespread. In 1969, pollution due to airforce aircrafts led to important federal laws on permissible sound/noise limitations in the US. Such laws led to the control of sound/noise output from various aircraft equipment. Since then, extensive studies have been conducted on aircraft noise (Ingard 2010).

However, with rapid advancements and developments of smart materials and intelligent control systems, wings with structured surfaces have become an attractive and ambitious concept being studied by many researchers. Especially, investigation of wings with structured surfaces performance and sound/noise control has attracted considerable attention.

One way to reduce sound/noise is to draw inspiration from birds (e.g., Owls). Sound/noise absorption of Owls' wings has been studied fairly well, resulting in unique characteristics, namely serrations at the leading edge (L.E.), sharp trailing edge (T.E.), and velvety upper surface (Kun *et al.* 2012). Some small birds, however, have corrugated shape wings, which have been proven to delay flow separation. Thus, humps on the T.E. area have more aerodynamic efficiency than on the L.E. region (Rohit *et al.* 2021 ; Shahzad *et al.* 2017). Note, morphing wings can also be substituted for aileron in wings (Previtali *et al.* 2014). Thus, using morphing wing increases maneuverability in which spanwise bending and twisting are effective (Joshi *et al.* 2020).

On the other hand, polymeric memory materials could be used for morphing wings. Such materials are able to reduce the overall mass of wings (Yazik and Sultan 2019; Tsushima 2020; Sneed 2007).

Morphing wings influence stall. The effects of T.E. morphing at different angles of attack on wing stall have been studied by Daochun *et al.* (2020). Their results show that such morphing and also morphing of chord line delay wing stall.

Gurvan *et al.* (2017) studied the dynamics of a flexible wing with vibrating T.E. (L.E. fixed/T.E. morphed) using time-resolved PIV and aerodynamic force measurement. Their wing was made of shaped memory material, and the actuators were piezoelectric. The effects of their wing on aerodynamic forces were measured, and optimal vibration amplitude was determined. As a result, they were able to significantly increase lift and decrease drag. Also, they studied the effects of high-frequency vibrations of the T.E. region. Their results indicate that vibrational frequency caused by a piezoelectric actuator at T.E. reduces drag and increases lift by forming effective eddies. Computational aeroacoustics has been developed to study many different applications (Zaini and Ismail 2016).

One state of morphing wing is changing the whole shape of airfoils (Dimino *et al.* 2017). There are six states of morphing wing as shown in Fig. 2 (Jawahar *et al.* 2020a) and Jawahar (2020b) and (Jawahar *et al.* 2018). An investigation of aerodynamics and aeroacoustics of a sweep, chord-wise and spanwise morphing wing was not reported in the past. In particular, there is a lack of studies on the aerodynamic and aeroacoustic analysis of morphing wings and wings with structured surfaces and serrated shapes (similar to Owl's wing) in the literature.

According to previous studies, using surface elements and serrations have been inspired by Owl's wings. Therefore, the dimensions used here for surface elements and serrations were taken from previous studies. However, the flow Reynolds number and the wing section used here are based on the characteristics of a certain class of UAV (for incompressible flow conditions) to make our studies more applicable. In addition, NACA2415 airfoil that has application in UAVs was selected for comparison purposes.

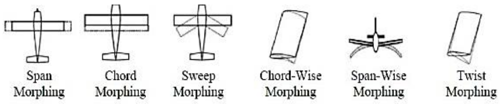

Fig. 1. Illustration of different types of morphing wing (Zaini and Ismail 2016).

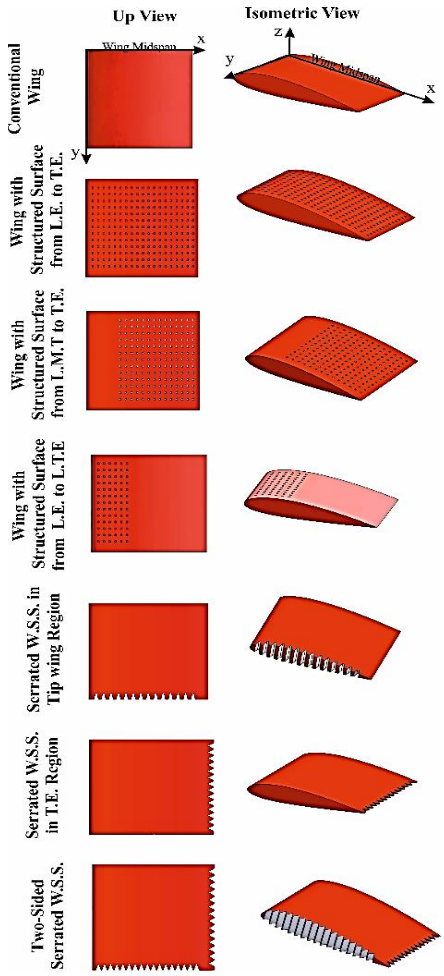

Fig. 2. Wing configurations studied here.

This work examines the aerodynamic and aeroacoustic of wings (without fuselage, but with origin of xyz coordinates at their midspans) with triangular, square, and semicircular surface elements and serrated shapes. Also, for more resemblance to Owl's wings, a combination of these elements with serrated shapes was studied.

2. METHODOLOGY

Figure 3 shows wings with different structured upper surfaces and various element distributions that are studied. These are: 1) from L.E. to T.E., 2) from L.E. to the location of the maximum thickness (L.M.T.), and 3) from L.M.T. to T.E. Reason for this design is that actuators, servo-motors, DC motors, etc. need enough spacing. Note, since using elements reduces the spacing inside the wing, which is usually used for equipment related to morphing mechanism, it is better to use elements in only parts of the wing (instead of everywhere on the wing).

Only square elements were displayed here. After examining the aerodynamic and aeroacoustic parameters of 13 different wings, the most suitable elements and their locations were selected. By combining the most suitable element and serrated shape, the optimal wing was selected from aerodynamic and aeroacoustic points of view.

As indicated in Fig. 4., based on typical Owl's wings, the distance between elements is 10 mm. Also, each element is extruded cut 2mm perpendicular to the surface of the wing. The circumference of each element is 20 mm. Each side of the square element is 5 mm, the triangular element is 6.66 mm, and the diameter of the semicircle element is 12.73 mm. As displayed in Fig. 5., the dimensions of serrated shapes are 20 mm on each side. Other parameters and assumptions made are:

- free stream velocity ≡ 50 m/s,
- Reynolds number ≡ 3.3e6,
- angle of attack ≡ 0 to 30,
- NACA2415 airfoil,
- chord line ≡ 40cm,
- wing span ≡ 60cm,
- fluid flow was assumed incompressible, non-stationary, and in the turbulent regime,
- gravitational effects are neglected.

3. GOVERNING EQUATIONS

A commercial CFD software (ANSYS-FLUENT) was used to simulate the flows around the wings in this study. For more accurate discretization of the equations, the MUSCL method was implemented.

3.1 k-ω SST Turbulence Model Equations

In Table 1, the predictions of different turbulence models for lift and drag coefficients are compared with the experimental data. This table shows that the k-ω SST is the most accurate model among the four tested. As shown in Fig. 5, k-ω B-L, k-ω SST, and Transition SST models produce very close values for sound power level (about 160 db). Thus, it can easily be concluded that any of these three models would be suitable to be used (k-ω SST was used here).

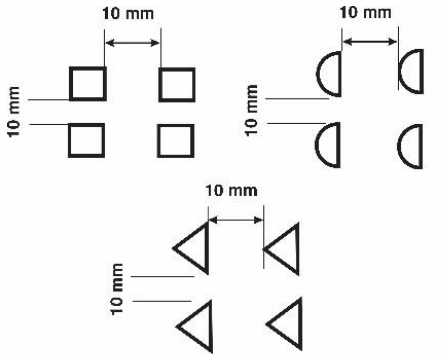

Fig. 3. Distances between elements used.

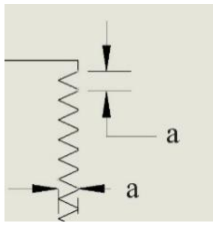

Fig. 4. Serrated shapes used (a is 20 mm).

Table 1 Comparison of simulated lift and drag coefficients for a conventional wing (NACA2415) at a zero angle of attack, using different turbulence models with the experimental data.

	Lift coefficient	Error percentage	Drag coefficient	Error percentage
Experimental results (Esmaeilpour 2010)	0.7017	-	0.0124	-
S-A	0.5312	26.91	0.0099	21.17
k-ε	0.5910	15.82	0.1030	16.94
k-ω B-L	0.6828	2.7	0.0120	3.23
k-ω SST	0.6992	0.36	0.0123	0.89
Transition SST	0.6992	0.37	0.0123	0.89

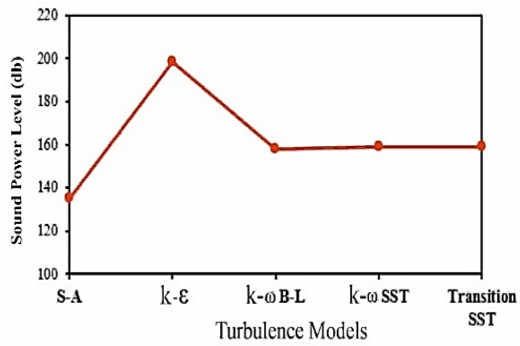

Fig. 5. Different examined turbulence models.

The two-equation eddy-viscosity k-ω SST model has become quite popular in recent years due to its adaptability during adverse pressure gradient and thus separation (Rohit *et al.* 2021). The corresponding model equations are given as:

$$\frac{\partial(\rho k)}{\partial t}+\frac{\partial(\rho u_j k)}{\partial x_j}=P-\beta^{*}\rho\omega k+\ldots$$
$$\ldots\frac{\partial}{\partial x_j}\left[(\mu+\sigma_k\mu_t)\frac{\partial(k)}{\partial x_j}\right], \tag{1}$$

$$\frac{\partial(\rho\omega)}{\partial t}+\frac{\partial(\rho u_j\omega)}{\partial x_j}=\frac{\gamma}{\nu_t}P-\beta^{*}\rho\omega^2+\ldots$$
$$\ldots\frac{\partial}{\partial x_j}\left[(\mu+\sigma_\omega\mu_t)\frac{\partial\omega}{\partial x_j}\right]+\ldots \tag{2}$$
$$\ldots 2(1-F_1)\left[\frac{\rho_{\omega^2}}{\omega}\frac{\partial(\rho\omega)}{\partial t}\frac{\partial(\rho k)}{\partial t}\right]$$

3.2 Aeroacoustic Relations

There are mainly two methods (direct and indirect) for aeroacoustic calculations. In the direct method, flow and aeroacoustic parameters are solved simultaneously. However, this method is considerably time-consuming. Lighthill (1952) proposed an indirect method, wherein flow and aeroacoustic relations are solved separately. That is, the flow and aeroacoustic computations are uncoupled. Here, variables like flow velocity and kinetic energy are computed using approaches like URANS, and then they are used to compute sound pressure. Proudman (1952) used Lighthill method to calculate acoustic power level for isotropic flow.

For a non-isotropic (general) turbulent flow using Navier-Stokes equations Lighthill derived an interesting equation relating sound to flowing motion. This equation was later named Lighthill analogy (Kim and Yoon 2020), as:

$$\frac{\partial^2\rho}{\partial t^2}-c^2\frac{\partial^2\rho}{\partial x_i\partial x_j}=\frac{\partial^2 T_{ij}}{\partial x_i\partial x_j}, \tag{3}$$

where,

$$T_{ij}=\rho v_i v_j+\left(p-c^2\rho\right)\delta_{ij}-\sigma_{ij}. \tag{4}$$

Note, several researchers have used the Lighthill analogy for cases close to ours, e.g., Jaworski *et al.* (2020).

4. Computational Simulation

The flow considered here was non-stationary and incompressible. The error criterion used in mass conservation was 10^{-3}, while it was 10^{-5} elsewhere.

4.1 Boundary Conditions

The boundary conditions used here were velocity-inlet and pressure outlet. In addition, no slip boundary condition was used at the wing surfaces.

4.2 Grid Resolution Study

A C-type grid was used for flow around wings. To ensure the grid independence of our numerical solution, different grid sizes were examined. Figure 6 shows the convergence of sound level (as a sensitive variable) at about 275,000 cells. In addition, aerodynamic efficiency was also computed for different number of cells. However, as shown in Fig. 7, convergence occurs at marginally smaller number of cells, assuring our previous grid independent study.

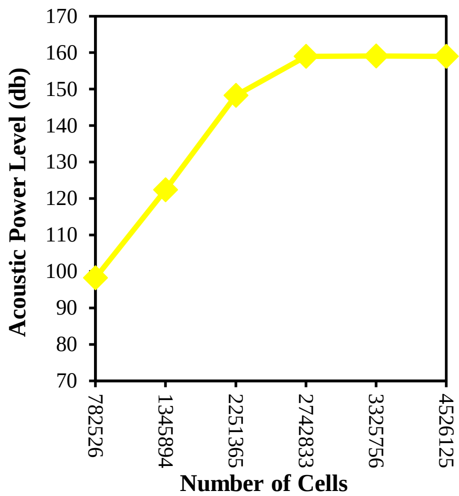

Fig. 6. Variation of acoustic power level with the number of cells used.

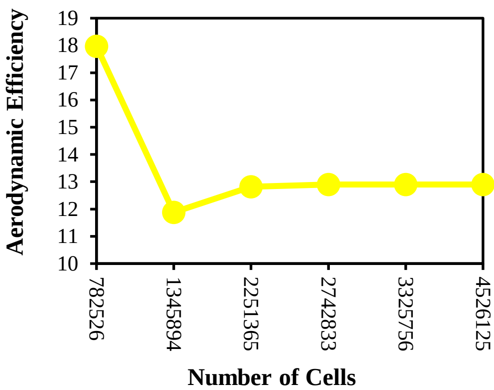

Fig. 7. Variation of aerodynamic efficiency with the number of cells used.

5. CODE VALIDATION STUDY

For validation purposes, our simulation results are compared with the experimental data of Ghods (2001), who studied a similar flow over a NACA2415 airfoil. As shown in Fig. 8, there is a relatively good agreement between the drag coefficient of the present study and the data of Ghods (2001). In addition, our results and the results of Genc *et al*. (2016) are compared in Fig. 9, showing close agreements.

6. RESULTS AND DISCUSSIONS

The lift coefficient for different elements used is shown in Fig. 10. This figure shows that the use of surface elements leads to delay in the stall and thus an increase in the maximum lift coefficient. The use of surface elements creates more turbulence, overcoming pressure increase in the T.E. region. Best performance is achieved for wings with square and semicircular elements. The optimal lift coefficient for all elements corresponds to the best performance in terms of delay in wing stall and is for the distribution of elements from L.M.T. to T.E. However, the use of elements on the whole wing (from L.E. to T.E.) has a poor performance. Note, the structured surface of Owls' wings also starts from about L.M.T., and thus, the use of structured surfaces seems appropriate for delaying wing stall.

Figure 11 displays the aerodynamic efficiency of the wing with surface structures. As shown in this figure, the wing with semicircular elements is able to reduce

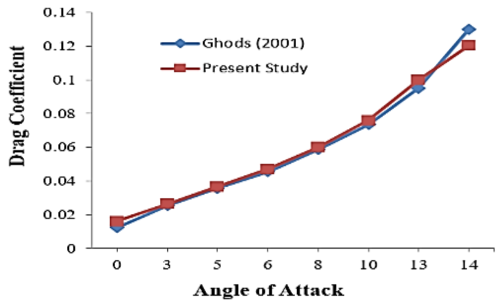

Fig. 8. Comparison of present results for drag coefficient (NACA2415 Airfoil) with previous experimental measurements (Ghods 2001).

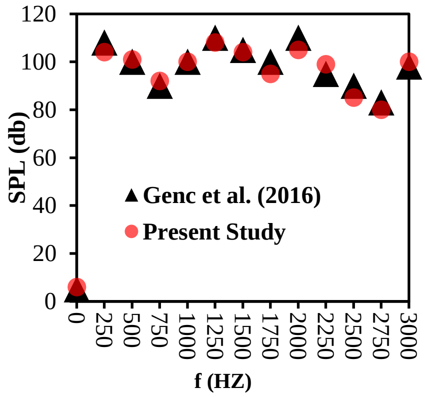

Fig. 9. Comparison between numerical computations (Genc *et al.* 2001) and present results for acoustic power level (NACA2415 Airfoil).

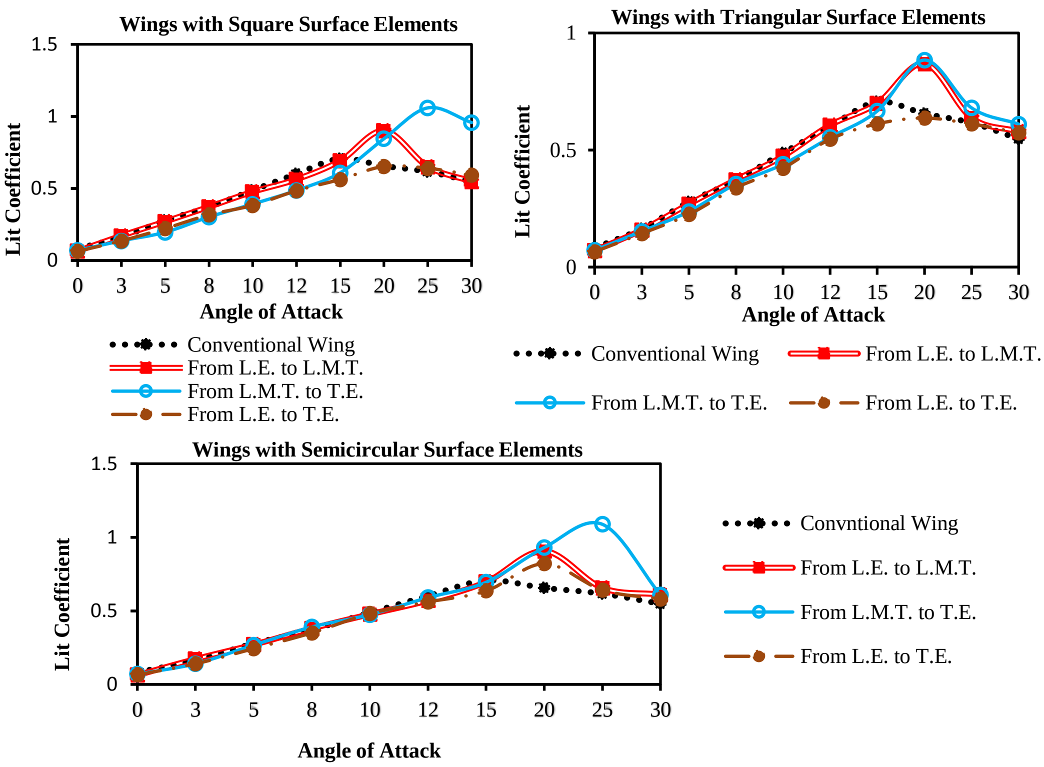

Fig. 10. Comparison of lift coefficient of a conventional wing with those of wings with different surface element.

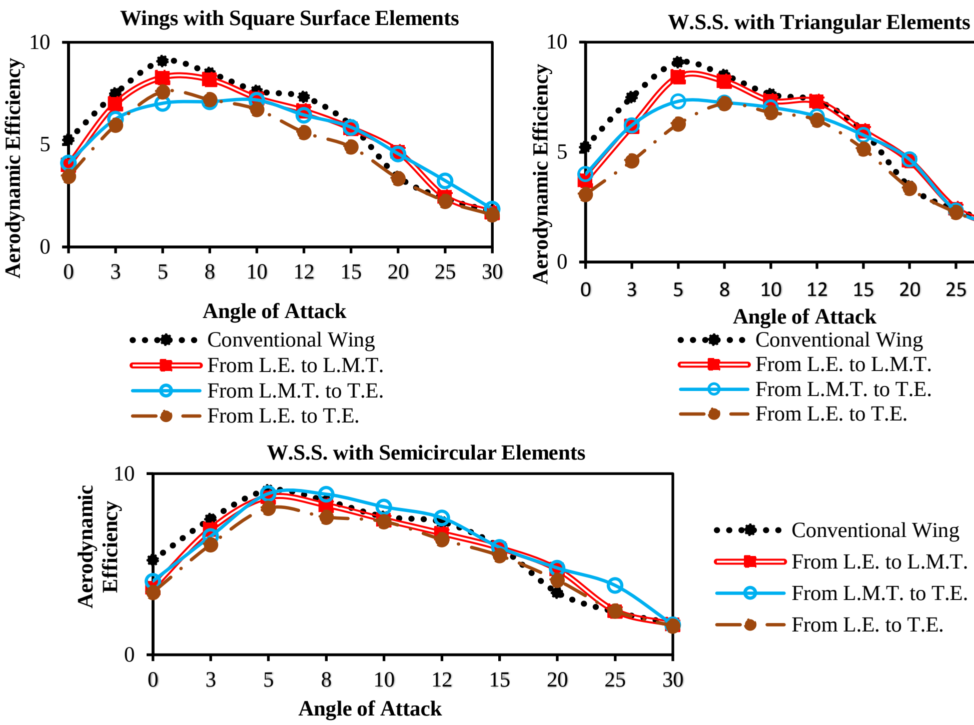

Fig. 11. Comparison of aerodynamic efficiency of a conventional wing with those of wings with different surface elements.

its wake region and thus its form drag after 5 degrees angle of attack. In addition, the aerodynamic efficiency of all wings with surface structures at angles of attack larger than 15 degrees is greater than that of a conventional wing.

The aeroacoustic results of a conventional wing are compared with those of wings with surface elements in Fig. 12. This figure shows that the sound produced increases with an increase in the angle of attack for all wings. As the angle of attack increases, the T.E. separation point on the top of the wing moves towards the L.E. Thus, the wake region enlarges. As a result, larger and more numerous vortices are created, producing stronger pressure pulses (leading to higher noise levels).

Another interesting result is comparing sound productions by different wings, using different surface elements and their various distributions on the wing. In addition, as indicated in Fig. 13, the sound propagation region becomes larger as the angle of attack increases, which leads to an increase in vorticity level. Note that the maximum sound level is produced in the compact region of vorticity. Therefore, there is a direct relationship between vortex generation and sound production.

For all angles of attack, the lowest sound level is associated with a wing with elements distributed from L.M.T. to T.E. This is because, by reducing the wake region due to the presence of elements, smaller and weaker vortices are being generated, leading to smaller pressure pulses and thus lower sound level. An Owl's wing's elements start approximately from L.M.T. Note that the elements distributed from L.E. to T.E. cause the generation of more vortices from L.E. of the wing, which transfer their energy to smaller vortices, and in more sound level. Therefore, turbulence reduces wake and thus reduces the production of sound. Therefore, the use of roughness or elements from L.E. to T.E. causes vortices from the beginning of the wing to produce more sound in an incompressible flow. Overally speaking, like elements used on Owls' wings, they significantly reduce sound production.

Figure 14 shows the results of aerodynamic and aeroacoustic simulations of serrated wings. The highest lift coefficient at all angles of attack is for the wing serrated in the T.E. region. Serration delays wing stall because it generates more turbulence, overcoming pressure increase in T.E. (up to about 25 degrees angle of attack). Thus, the wake region becomes smaller, and the lift coefficient (and aerodynamic efficiency) for two-sided serrated wings increase. Note that in Owl's wings, serrations are larger in the L.E. region than in the T.E area. This is probably why aerodynamic efficiency for a two-sided serrated W.S.S. is less than that of a serrated wing. As displayed in this figure, the lowest sound level among all angles of attack is for a two-sided serrated wing. Also, the highest one is for the serrated wing in the T.E. region.

Thus, different wings with structured surfaces with elements from L.M.T. to T.E. have the most appropriate lift coefficients. Furthermore, to improve aerodynamic efficiency, wing stall needs to be delayed. Therefore, a wing with surface elements from L.M.T. to T.E. has the most appropriate aerodynamic efficiency. Such a wing also has the least sound level. Therefore, the use of surface elements from L.M.T. to T.E. is most appropriate.

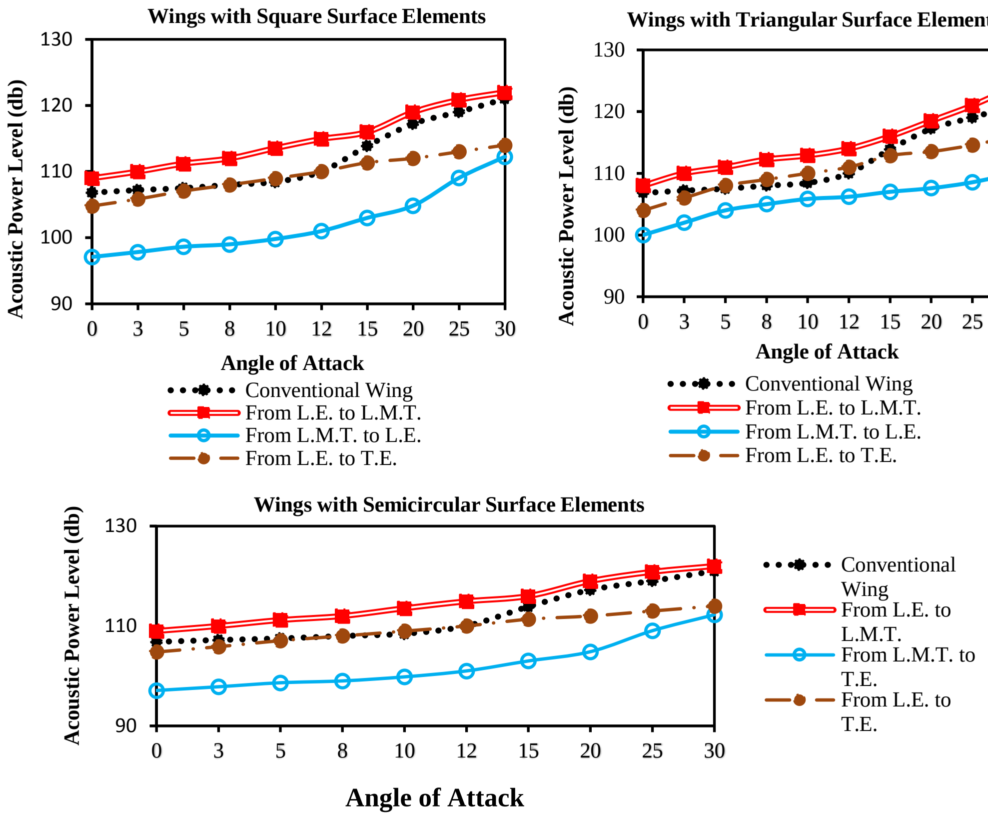

Fig. 12. Comparison of the acoustic power level of a conventional wing with those of wings with different surface elements.

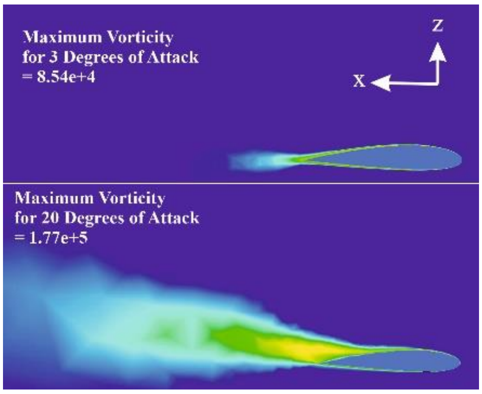

Fig. 13. Sound propagation region of a conventional wing at two different angles of attack.

As illustrated in Fig. 15, from an angle of attack greater than about 15, the use of surface elements and serrations delay the wing stall. Also, at all angles of attack, the highest lift coefficients belong to the wing serrated in the T.E. region. However, the lift coefficient at zero angle of attack is the same for all wings because they all have the same camber line.

Figure 16 shows the aerodynamic efficiency of different wings studied here. At angles of attack greater than about 15 degrees, the lowest efficiency is seen for a conventional wing. This is because stall occurs at about this angle. At angles of attack between about 5 and 15 degrees, the highest efficiency belongs to the wing with semicircular elements distributed from L.M.T. to T.E. due to higher turbulence.

Another exciting result is reducing the produced sound by using both surface elements and serrations (Fig. 17). In other words, inspired by Owl-shaped wings, the sound is considerably reduced. This is the result of important factors like an increase in turbulence and a decrease in wake region. Finally, wings with square elements from L.M.T. to the T.E. and serrated W.S.S. in the T.E. region have the lowest sound level at almost all angles of attack studied here.

As shown in Fig. 18a, wings with elements produce sound in smaller regions compared to a plain wing. This is due to the fact that elements cause more disturbances leading to enhancement of turbulence, which means less boundary layer growth and thus less vortical regions causing sound.

Figure 18b shows vorticity shadowgraph of flow or different wings. As expected, there are considerably more vortical flow near wing L.E. and wing tips. Note, vorticity generation is directly related to production of sound. Thus, there are usually more sound generation at these two locations. Comparing the five test cases studied here, the ones which have been able to reduce vortex generation at these two locations perform better as far as reduction of sound is concerned.

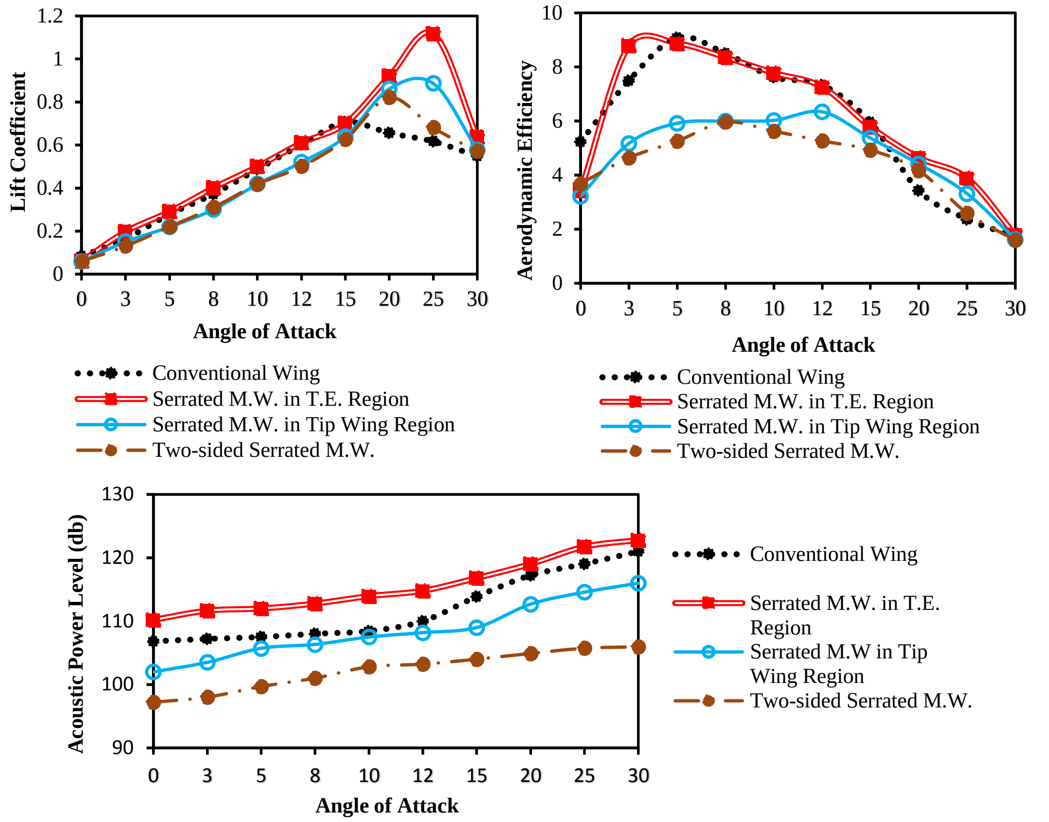

Fig. 14. Comparison of aeroacoustic and aerodynamic parameters for a conventional wing with those of serrated wings.

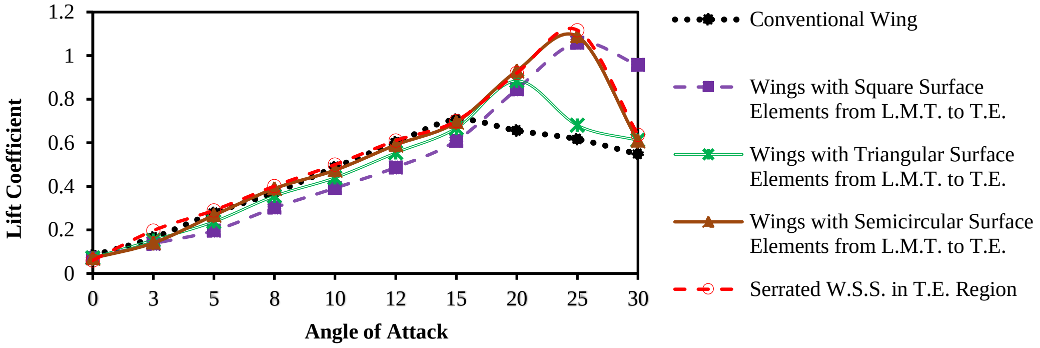

Fig. 15. Comparison of lift coefficient for a conventional wing with those of wings with different surface elements and with and various distributions.

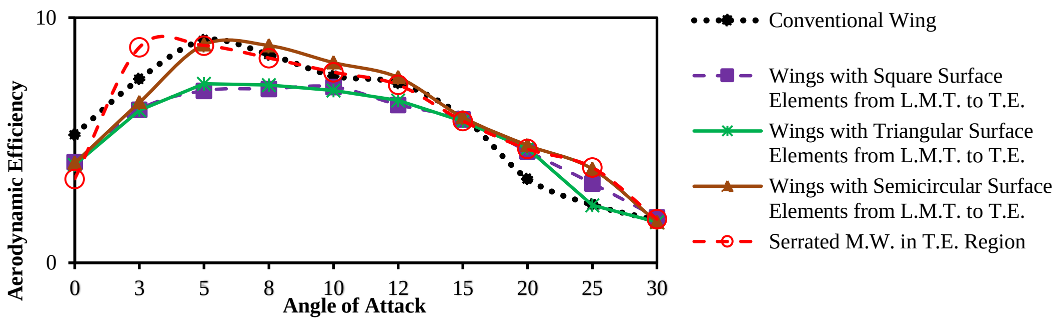

Fig. 16. Comparison of aerodynamic efficiency for a conventional wing with those of wings with different surface elements and various distributions.

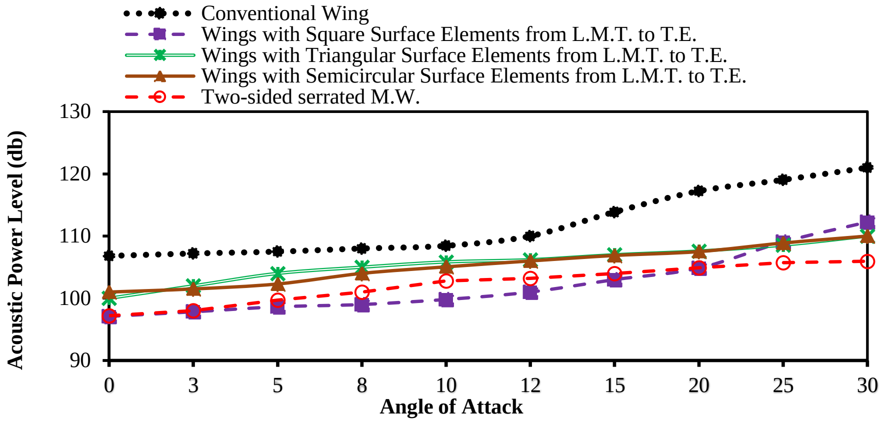

Fig. 17. Comparison of acoustic power level for a conventional wing with those of wings with different surface elements and various distributions.

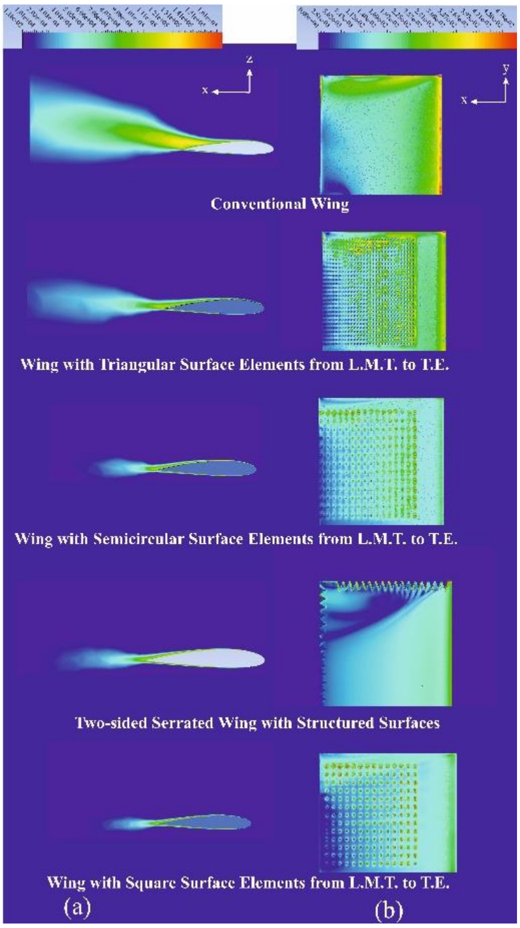

Fig. 18. Sound and flow over a conventional wing and over wings with different surface elements (at different locations) for 10 degrees angle of attack, using shadowgraphs of (a) mean sound pressure (dB) (at wing midspan) (b) mean vorticity (1/s).

7. CONCLUSIONS

In this study, aerodynamic and aeroacoustic parameters of wings with square, triangular, and semicircular surface elements and different serrations were studied. The following conclusions are made:

1- Surface elements and serrations significantly affect the wing aerodynamic and aeroacoustic performance, starting at about 15 degrees angle of attack. They delay wing stall (by an average of about 25%) and thus increase the maximum lift coefficient (average of about 20%).

2- To improve aerodynamic and aeroacoustic characteristics, it is appropriate to distribute the surface elements from L.M.T. to T.E. (like in Owls' wings).
3- Square and semicircular surface elements are most effective for improving the aerodynamic and aeroacoustic performance of wings.

As the future outlook of this work, one can provide a physical explanation for why wing with semicircular surface elements and serrated wing with structured surfaces in T.E. region perform much better in aerodynamic efficiency than wing with square and triangular surface elements. Similarly, he/she can provide a physical explanation for why wing with semicircular surface elements perform much worse in acoustic power level than wing with square surface elements and why, despite very different aerodynamic efficiency between wing with semicircular and triangular surface elements, their acoustic performance is similar. In addition, it can be investigated why serrated wing with structured elements in T.E. region and with similar aerodynamic performance as wing with semicircular surface elements performs a lot worse in acoustic power level.

REFERENCES

Daochun, K.Z., L.J. Xiang and C. Cheng (2020). *Chinese Journal of Aeronautics* 33(2), 493-500.

Dimino, I., L. Lecce and D. R, Pecora (2017). Morphing Wing Technologies: Large Commercial Aircraft and Civil Helicopters Butterworth-Heinemann, Oxford, United Kingdom.

Esmaeilpour, M. (2010). *Asseeement of B-L, k-Omega, k-epsilon, SST Turbulent Models for External Flow over an Airfoil*. M.Sc. Thesis, Mechanical Engineering Department, Sharif University of Technology, Tehran, Iran.

Genç, M. S., İ. Karasu, H. H. Açıkel, M. T. Akpolat and G. Özkan (2016). Acoustic Control of Flow over NACA2415 Airofoil at Low Reynolds Numbers. *Sustainable Aviation* 29(6), 375-420.

Ghods, M. (2001). *Theory of Wings and Wind Tunnel Testing of a NACA2415 Airfoil*. Ph.D. Dissertation, Aerspace Engineering Department, University of British Columbia, Vancouver, Canada.

Gurvan, J. M., S. Valentina, D. Johannes, E. D. Carsten, R. Jean-François and B. Marianna (2017). Dynamics of a Hybrid Morphing Wing with Active Open Loop Vibrating Trailing Edge by Time-resolved PIV and Force Measurements. *Journal of Fluids and Structures* 74(12), 263-290.

Ingard, U. (2010). *Notes on Acoustics*. Jones & Bartlett Massachusetts, USA.

Jawahar, H. Kamliya. and M. Azarpeyvand (2018). Aerodynamic and Aeroacoustic Performance of Airfoils Fitted with Morphing Trailing-edges. AIAA/CEAS Aeroacoustics Conference, University of Bristol, Princeton, *AIAA/CEAS Aeroacoustics Conference*, University of Bristol, Princeton, U.S.A.

Jawahar, H. K., N. Zang and M. Azarpeyvand (2020a). Aerodynamic and Aeroacoustic Performance of Spanwise Morphed Airfoils. *AIAA Aviation Forum* 100, 2580.

Jawahar, H. K., M. Azarpeyvand and C. Ilario (2020b). Aerodynamic and Aeroacoustic Performance of High-lift Airfoil with Serrated Slat Cusp. *AIAA Aviation Forum* 2554.

Jaworski, J. W. and N. Peake (2020). Aeroacoustics of Silent Owl Flight. *Annual Review of Fluid Mechanics* 52, 395-420.

Joshi, K., C. G. Vazquez, J. L. Kauffman and S. Bhattacharya (2020). Unsteady Maneuvering of a Morphing Wing. *AIAA Scitech* 185-193.

Kim, K. J. and G. H. Yoon (2020). Aeroacoustic Topology Optimization of Noise Barrier, Based on Lighthill's Acoustic Analogy. *Journal of Sound and Vibration* 483, 1-27.

Kun, C., L. Qingping and L. Genghua (2012). The Sound Suppression Characteristics of Wing Feather of Owl (Bubo Bubo). *Journal of Bionic Engineering* 9(2), 192-199.

Lighthill, M. J. (1952). On Sound Generated Aerodynamically I. General Theory. The Royal Society of London. Series A. *Mathematical and Physical Sciences* 211(1107), 564-587.

Previtali, F. M., A. F. Arrieta and P. Emadi (2014). Performance of a Three-dimensional Morphing Wing and Comparison with a Conventional Wing. *AIAA J* 52(10), 883-845.

Proudman, I. (1952). The Generation of Noise by Isotropic Turbulence. Royal Society of London. *Series A. Mathematical and Physical Sciences* 214(1116), 119-132.

Rohit, B., S. S. R. Redy, S. Ghosh and S. Shakil (2021). Computations of Flow Past the Corrugated Sirfoil of Drosophila Melanogaster at Ultra Low Reynolds Number. *Journal of Applied Fluid Mechanics* 14(2), 417-427.

Shahzad, A., H. Hamdani and A. Aizaz (2017). Investigation of Corrugated Wing in Unsteady Motion. *Journal of Applied Fluid Mechanics* 10(3), 833-845.

Sneed, N., R. Smith, M. Cash and E. Anderson (2007). Smart-material Based Hydraulic Pump System for Actuation of a Morphing Wing. The 48th AIAA/ASME/ASCE/ AHS/ASC Structures, Structural Dynamics, and Materials Conference, University of Hawaii, Hawaii, U.S.A.

Tsushima, R., M. Tamayama and H. Arizono (2020). Aeroelastic Characteristics of Morphing Wings with Pantographic Substructures. *AIAA Scitech* 2020, 2189.

Yazik, M. M. and M. Sultan (2019). Shape Memory Polymer and Its Composites as Morphing Materials. Failure Analysis in Biocomposites, Fibre-Reinforced Composites and Hybrid Composites. *Elsevier*, 181-198.

Zaini, H. and N. Ismail (2016). A Review of Morphing Wings. International Conference in Mechanical Engineering Colloquium, School of Mechanical Engineering, University of Liverpool, Liverpool, England.